GMR

The Original

QUANTUM INSPIRED HYPERPARAMETER TUNING OPTIMIZATION FOR COMPUTATIONAL PREDICTION OF MENTAL HEALTH DISORDERS

Ashok Kumar Panigrahi[1], Chittaranjan Mallick[2], Kalyan Kumar Jena[3*]

[1]Faculty of Computer Application and Sciences, Biju Patnaik University of Technology, Rourkela, 769015, Odisha, India, Email: ashokpanigrahimath@gmail.com, http://orcid.org/0009-0003-0664-5010
[2]Department of Mathematics, Parala Maharaja Engineering College, Berhampur, Odisha, India, Email: cmallick75@gmail.com, http://orcid.org/ 0000-0002-4165-652X
[3]Department of Computer Science and Engineering, Parala Maharaja Engineering College, Berhampur, Odisha, India, Email: kalyankumarjena1@gmail.com, http://orcid.org/ 0000-0002-2476-5644

ABSTRACT
Mental health has a deep effect on human health affecting individuals in physically, emotionally and socially. Poor mental health can lead to numerous physical, emotional and behavioral consequences which can significantly impact overall health and quality of life. So, Mental health disorders (MHD) prediction is essential in the field of research for early identification and intervention, improving treatment efficacy, reducing stigma, improving quality of life, addressing Comorbidities, etc. The Mental Health Disorders (MHD) can be tracked using a range of methods including: Quantum Computing (QC), Federated Learning (FL), Machine Learning (ML), Deep Learning (DL), and Edge Computing. In this study we focus on the use of Quantum ML (QML) to predict MHD as Anxiety (AX), Depression (DP), Loneliness (LL), Stress (ST), or Normal (NR). For this study we will evaluate three models: Quantum Gradient Boosting (QGB); Quantum Support Vector Machine (QSM); and Hybrid Quantum Classical Model (HQM). Each model will be compared based on Accuracy (A in %); Precision (P in %); Recall (R in %); F1 Score(F1S in %); Training time (TT in secs); Memory Usage (M in MB); & Model Size (MS in KB) with 80:20, 70:30, & 60:40 Training Testing Ratios (TTR in \%) before and after applying Grid Search (GS) based Hyperparameter (HP) Tuning (HPT) optimization to identify if there is a statistically significant improvement in performance. Additionally, the receiver operating characteristic (ROC) curve will provide TPR & FPR for each model; while Boxplot & Heatmaps will visually represent these parameters. Analysis of results show that the performance of HQM is higher on average (A, P, R, F1S) than A, P and TT with averages of 94.1, 94.0, 94.1, 94.2 and 4.49 for both HQM before and HQM after HPT testing. However, QSM performs better in terms of M and MS with values 1274.41 and 88.54, and 1269.36 and 80.53 accordingly.

KEYWORDS: Quantum Machine Learning, Mental Health Disorders, Hyperparameter Tuning, Classification Accuracy, Precision, Recall, Training Time, Memory Usage, Model Size

1. INTRODUCTION

Mental health plays a crucial role in overall well being notably impacting various aspects of human health. It affects how individuals think, feel and act, and has a strong influence on physical health, emotional stability and social interactions. So, it is very much important to keep mental health condition as NR to avoid adverse effects on human health. MHD [1-10] refers to a wide variety of conditions which affect an individual's thoughts, emotions, behavior and overall functioning. It can cause distress and disrupt daily life, relationships and the capability to perform normal activities. MHD can affect people of all ages. Different types of MHD include AX, DP, LL, ST, Mood, psychotic, personality, neuro-developmental, eating, obsessive compulsive, etc. The causes influencing MHD are genetics, chronic health conditions, psychological factors, environmental factors, biological factors, etc. It has impact on physical health such as immune system, chronic diseases, sleep disruptions, etc., emotional stability such as emotional regulation and self-esteem, social interactions such as interactions and Communication, hormonal and neurological such as brain chemistry, behavior and lifestyle such as social isolation, etc. However, the treatments such as medications, psychotherapy, lifestyle change, etc. can lower the MHD conditions. So, MHD prediction is essential in the field of research for early identification and intervention, improving treatment efficacy, reducing stigma, improving quality of life, addressing Comorbidities, etc. Tracking the MHD condition with Multiple Techniques such as ML, DL, QML, FL etc. can be done via various methods. MHD condition monitoring [11-20] can be done via several ML Models and DL models. MHD condition monitoring can also be done via QML Techniques such as Quantum State Measurement (QSM), Quantum Neural Network (QNN), Quantum Gradient Boosting (QGB), Hexagonal Kernel Maps (HQM) etc. MHD Condition Monitoring can also be done via FL Models such as Federated Averaging, Federated Stochastic Gradient Descent, Federated Multi-Task Learning etc. Apart from these methods some other methods which can be used for such purpose are genetic algorithms, swarm intelligence, etc.

This paper concentrates on the significant QML [21-27] advantages such as handling of high-dimensional data comparatively well, applying improved methods to feature extraction and classification, executing fast calculation methods, dealing with noisy data optimally, optimising predictive maintenance, dealing with complex classification problems, improving fault diagnosis accuracy and how quantum-based QML methods such as QGB, QSM and HQM will allow for improved and faster condition prediction of MHD by providing enhanced performance and accelerated calculation using quantum superposition/entanglement to facilitate analysis of multiple possibilities simultaneously, therefore significantly improving the classification process; allowing for detection of subtle patterns in the data that traditional ML would Not be able to identify; and subsequently allowing for more accurate and timely identification of potential problems thereby further improving predictive capability of MHD conditions. A unique motivation for adopting a QML-based approach for MHD classification is to enhance the efficiency, predictive accuracy, and scalability of MHD monitoring systems by leveraging the computational capabilities offered by QC. However, classical ML often struggles to handle large scale, high dimensional data in the real world scenarios whereas QC based approach offers the ability to process data in parallel and capture complex as well as nonlinear relationships in an effective manner. It is also able to handle uncertainty and noisy data, adjust to dynamic operational conditions and improve the feature selection which leads to enhancement of the overall A. In this study, a foundation is established for using rating models to assess the effects of MHD on a number of conditions including AX, DP, LL, ST and NR. A number of methods are developed based on QGB, QSM and HQM to perform this analysis, and the models are compared using the mentioned performance metrics. The detailed results from this analysis are illustrated using ROC Curves, Boxplots, and Heatmaps.

The major contributions and findings from this study are detailed below.

- The use of QML based rating models for MHD prediction is established as a new approach.
- QGB, QSM and HQM models are developed to evaluate MHD.
- Models are compared across performance metrics A, P, R, F1S, TT, M, MS with TTR as 80:20, 70:30, and 60:40 pre/post- HPT application.
- The result shows a ROC curve, boxplot and heatmap graphs that have been plotted with an emphasis on these values to visualize how HPT affects the results.
- According to the results obtained, on average, HQM shows better performance values than A, P and R as referred to in the next sections, i.e., A = 94.1, P = 94.0, R = 94.1, F1S = 94.2, and TT = 4.49 and before and after HPT, A = 96.9, P = 96.8, R = 96.8, F1S = 96.8, and TT = 4.35.
- However, QSM performs better in terms of of M and MS with values 1274.41 and 88.54, and 1269.36 and 80.53 accordingly.
- These results are produced using Jupyter Notebook 7.2.1.

In the following work, we have outlined the remaining sections as follows. Sections 2 to 7 cover the literature review, problem description, methodology, results and discussion, statistical analysis and conclusion accordingly.

2. RELATED WORKS

Many research has been done concerning QML [1-27]. Several relevant works are presented below. Manocha et al. [1] focused on a framework inspired by the Internet of Things (IoT) for monitoring behavior to assess panic disorder within a specific context. This framework utilizes a quantum probability based quantification method to evaluate the extent of health abnormalities. Here, temporal data mining (TDM) is applied to generate temporal data granules, enabling the calculation of the individual health index (IHI) using the multi scaled gated recurrent unit (M-GRU) DL technique. Again, a two phase alert system is proposed to notify the relevant caretaker or medical professional about the individual's current health status by facilitating timely medical or assistive intervention. Singh et al. [2] provides a comparative analysis of various ST detection techniques using EEG signals by focusing on quantum inspired methods. Here, a real time neurofeedback solution based on quantum computing principles is introduced to offer a quantitative evaluation of ST levels. By incorporating QC concepts into both ST detection and management, this work contributes to individual health and has broader implications for ST related mental health and clinical practices. Again, it pushes the boundaries of neuroethology by exploring the intersection of quantum technology and cognitive health. In their research, Goswani et al. [3] specialize in investigating the unique qualitative features of quantum artificial intelligence (AI) algorithms and their ability to process complex healthcare data efficiently. They demonstrate that these algorithms take advantage of the fundamentals of quantum physics, such as superposition and entanglement, to exceed the limits of traditional AI techniques. The researchers also address how quantum AI can be integrated into existing healthcare technologies by reviewing the potential of these technologies in areas such as predictive analysis, customized treatment plans, and precision medicine. Ethical concerns around quantum AI and privacy issues will also be covered, along with the potential of combining quantum intelligence and healthcare. In this context, Shahwar et al. [4] discuss the use of deep learning (DL) models for classifying Alzheimer's disease using a convolutional neural network (CNN). They highlight that MRI scans can assist in identifying early indicators of Alzheimer's disease and further propose a hybrid classical–quantum transfer learning framework for detecting Alzheimer's disease from brain MRI images. Finally, they suggest that variational quantum circuits can be implemented to convert input data into a quantum circuit to use with ResNet34 as a pre-trained CNN and with a quantum model to classify Alzheimer's disease. Prior to Padha et al. [5]'s research, several types of classical ML models were developed that added quantum enhancements and assessed the levels of performance based on predictions made from time series-based multimodal mental state tracking data collected through various methods. Furthermore, once the time series data had been collected, they used principal component analysis (PCA) on the high-dimensional data to show diversity and find strong relationships with QML models through pattern identification. Finally, a meta methodology was established to unify the prediction abilities of several QMLs (built using the same amplified variance) to increase the overall performance of the combined QMLs.

There are several research areas that needed development indicated by the analyses of the different approaches. Some of these research gaps include: not enough research on quantum-algorithm based MHD predictors, insufficient use of quantum feature mapping for large datasets, not enough emphasis on integrating QML models for problem-related prediction applications, etc.. To address these issues will require development of improved quantum-based methods.

3. PROBLEM STATEMENT

Using the QML-based method to predict MHD is a classification problem. That is, the goal is to predict the individual's health status (NR or not NR) based on the data collected for that individual. The collected data is represented as $X = \{x_1, x_2, \ldots, x_n\}$, where each xi is a feature vector that contains sensor readings (temperature, pressure, vibration) and has multiple dimensions based on the number of measurements taken. Each feature vector has an associated output value denoted by $y_i \in \{0, 1\}$ with 0 corresponding to NR and 1 corresponding to not NR (AX, DP, LL, ST, etc.).

4. METHODOLOGY

This study describes all of the methods that will be used to do the experiment shown in Figure 1. The data used for the experiment dataset (D) comes from source [28]. The D is preprocessed by replacing missing values with the mean of the corresponding feature and normalizing the data using the Z-score method. After preparation, the D is transformed to a lower dimensional space through PCA. After transforming the original D, the QML are executed on D to evaluate the models' performance on A, P, R, F1, TT, M and MS. The TTR be set at 80%/20%, 70%/30%, and 60%/40%, respectively, over the D. The ROC curve is drawn with TPR and FPR data for each individual model, and the boxplots and heatmaps will be drawn based on the former metrics. Lastly, the MHD classification will be split into AX, DP, LL, ST, and NR.

4.1 PROPOSED APPROACH

This approach takes some classification data and goes through several different preprocessing steps including imputation of missing values by taking the mean by feature and normalizing the classification data into a distribution using the Z-score method. Following this preprocessing, PCA will be applied to obtain fewer features. The number of features created from this PCA operation will correspond to the number of NQ used in the quantum circuit to represent how classical features can be transformed into quantum states. Using machine learning algorithms to perform classification on the quantum data will be accomplished using QGB, QSM, and HQM (Stacking) models and will be part of this analysis. The QGB, QSM, and HQM (no HPT) algorithms and QGB, QSM, and HQM (with HPT) algorithms are detailed in Algorithms 1-6.

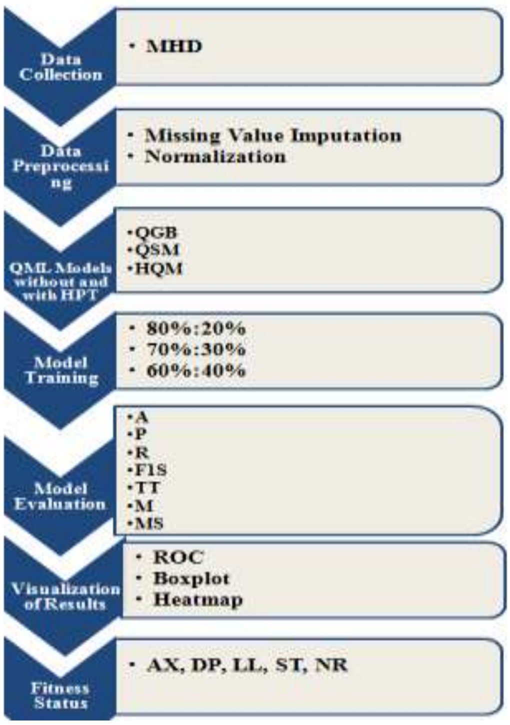

Figure 1: Methodology

Algorithm 1: QGB without HPT
Input: **D, NQ, Test Size**
Output: **A, P, R, F1S, TT, M, MS**
1: Load D with feature set X and labels Y.
2: For each feature in X:
• Apply mean value imputation.
• Apply Z-score normalization.
3: Generate Normalized_X.
4: Apply PCA on Normalized_X with ND = NQ.
5: Apply QF to obtain QF.
6: Split QF and Y into Xtrain, Xtest, Ytrain, and Ytest.
7: Train QGB classifier using Xtrain and Ytrain.
8: Predict Y using Xtest.
9: Compute Metrices.

Algorithm 2: QSM without HPT
Input: D, NQ, Test Size
Output: A, P, R, F1S, TT, M, MS
1: Load D with feature set X and labels Y.
2: For each feature in X:
• Apply mean value imputation.
• Apply Z-score normalization.
3: Generate Normalized_X.
4: Apply PCA on Normalized_X with ND = NQ.
5: Apply QF to obtain QF.
6: Split QF and Y into Xtrain, Xtest, Ytrain, and Ytest.
7: Train QSM using linear SVM.
8: Predict Y using Xtest.
9: Compute Metrices.

Algorithm 3: HQM without HPT
Input: D, NQ, Test Size
Output: A, P, R, F1S, TT, M, MS
1: Load D with feature set X and labels Y.
2: For each feature in X:
• Apply mean value imputation.
• Apply Z-score normalization.
3: Generate Normalized_X.
4: Apply PCA on Normalized_X with ND = NQ.
5: Apply QF to obtain QF.
6: Split QF and Y into Xtrain, Xtest, Ytrain, and Ytest.
7: Train CGB.
8: Construct HQM using:
• Base Learners: CGB and QGB
• Meta Model: LR
9: Train HQM.
10: Predict Y using Xtest.
11: Compute Metrices.

Algorithm 4: QGB with HPT
Input: D, NQ, Test Size, HP Grid
Output: A, P, R, F1S, TT, M, MS
1: Load D with feature set X and labels Y.
2: For each feature in X:
• Apply mean value imputation.
• Apply Z-score normalization.
3: Generate Normalized_X.
4: Apply PCA on Normalized_X with ND = NQ.
5: Apply QF to obtain QF.
6: Split QF and Y into Xtrain, Xtest, Ytrain, and Ytest.
7: Define HP Grid.
8: Apply GSCV to identify optimal HPs.
9: Train UpdatedQGB using optimal HPs.
10: Predict Y using Xtest.
11: Compute Metrices.

Algorithm 5: QSM with HPT
Input: D, NQ, Test Size, HP Grid
Output: A, P, R, F1S, TT, M, MS
1: Load D with feature set X and labels Y.
2: For each feature in X:
• Apply mean value imputation.
• Apply Z-score normalization.
3: Generate Normalized_X.
4: Apply PCA on Normalized_X with ND = NQ.
5: Apply QF to obtain QF.
6: Split QF and Y into Xtrain, Xtest, Ytrain, and Ytest.
7: Define HP Grid.
8: Apply GSCV to identify optimal HPs.
9: Train UpdatedQSM using optimal HPs.
10: Predict Y using Xtest.
11: Compute Metrices.

Algorithm 6: HQM with HPT
Input: D, NQ, Test Size, HP Grid
Output: A, P, R, F1S, TT, M, MS
1: Load D with feature set X and labels Y.
2: For each feature in X:
• Apply mean value imputation.
• Apply Z-score normalization.
3: Generate Normalized_X.
4: Apply PCA on Normalized_X with ND = NQ.
5: Apply QF to obtain QF.
6: Split QF and Y into Xtrain, Xtest, Ytrain, and Ytest.
7: Define HP Grid.
8: Apply GSCV to identify optimal HPs.
9: Train UpdatedHQM using optimal HPs.
10: Construct UpdatedHQM using:
• Base Learners: CGB and UpdatedQGB
• Meta Model: LR
11: Train UpdatedHQM.
12: Predict Y using Xtest.
13: Compute Metrices.

4.2 PROPOSED APPROACH

4.2 .1 Input Data Representation

The dataset consists of n samples and m features. Each sample contains multiple attributes used for MHD prediction, while the corresponding label indicates the class category. The dataset and labels are represented as follows:

Dataset:

$X = [x_1, x_2, x_3, ...]$

Labels:

$Y = [y_1, y_2, y_3, ...]$

where $y_i \in \{0,1\}$.

4.2 .2 Data Preprocessing

Data preprocessing is carried out to enhance data quality and improve model performance. Missing values are handled and all features are normalized to ensure consistent scaling across the dataset.

4.2 .2.1 Missing Value Imputation

Missing values are replaced using the mean of the available values in the corresponding feature.

Missing Value = (Sum of Available Values)/(Number of Available Values) (1)

4.2 .2.2 Z-Score Normalization

Normalization transforms feature values into a common scale with zero mean and unit variance.

Z = (X − Mean)/Standard Deviation   (2)

4.2 .2.3 PCA-Based Dimensionality Reduction

PCA is applied when the number of features exceeds the number of qubits. It reduces dimensionality while preserving the most important information from the dataset.

XPCA = PCA(Xscaled)   (3)

4.2.3 **Quantum Feature Mapping**
The reduced feature set is transformed into a quantum feature space using a quantum feature map. This process allows the model to capture complex feature relationships in a higher-dimensional quantum representation.
Qi = MQ(Xi)   (4)
4.2.4 **Train-Test Split**
The processed dataset is partitioned into training and testing subsets. The training subset is utilized for model development, whereas the testing subset is employed to assess model performance.
D = Train Data + Test Data   (5)
4.2.5 **QGB Model**
QGB combines quantum feature mapping with Gradient Boosting to perform classification. Multiple weak learners are sequentially trained to improve prediction accuracy.
QGB = Train(Xtrain, Ytrain) (6)
Prediction: P = QGB(Xtest)   (7)
4.2.6 **QSM Model**
QSM utilizes quantum-enhanced features with an SVM classifier. The model identifies optimal decision boundaries in the transformed quantum feature space.
QSM = Train(Xtrain, Ytrain) (8)
Prediction: P = QSM(Xtest) (9)
4.2.7 **HQM Model**
HQM combines classical and quantum learning approaches through a stacking framework. Predictions from multiple base learners are integrated using a meta-classifier to improve overall performance.
P_1 = CGB(X) (10)
P_2 = QGB(X)   (11)
Final Prediction: PHQM = LR(P_1,P_2)   (12)
4.2.8 **HPT**
HPT is used to identify the best parameter values for each model. Grid Search and Cross Validation are employed to evaluate multiple parameter combinations and select the optimal configuration.
Parameter Grid: PG = {HP_1, HP_2, HP_3, ...}   (13)
4.2.9 **Cross Validation Score**
Cross Validation evaluates model performance across multiple folds and reduces the risk of overfitting. The average score obtained from all folds is used as the final evaluation metric.
$F = (F_1 + F_2 + ... + F_k)/k$ (14)
4.2.10 **Optimal Hyperparameters**
The parameter combination producing the highest validation score is selected as the optimal configuration for the model.
$\lambda^* = \text{argmax}(F)$ (15)
4.2.11 **Optimized Model**
After selecting the optimal hyperparameters, the final model is retrained using the entire training dataset. The optimized model is then used for prediction and evaluation.
Optimal Model = Best Estimator   (16)

5. RESULTS AND DISCUSSION

This work is done using Jupyter Notebook 7.2.1. Here, the D is taken from the source [28] for processing. The QML models such as QGB, QSM and HQM are analyzed using the TTR such as 80%:20%, 70%:30% and 60%:40%. The performance of these models is assessed based on the discussed parameters. The performance of these models is also visualized using ROC curve, boxplot and heatmap representation. The results of several methods by considering the TTR as 80%:20%, 70%:30% and 60%:40% by considering before and after HPT are mentioned in Table 1- Table 6.

Table 1: Results of several methods at 80 : 20 TTR before HPT

Model	A	P	R	F1S	TT	M	MS
QGB	93.70	93.69	93.79	93.62	127.82	1285.19	178.39
QSM	90.29	90.37	90.24	89.71	115.1928	1276.69	89.47
HQM	95.54	95.49	95.50	95.42	4.56	2335.48	528.53

Table 2: Results of several methods at 80 : 20 TTR after HPT

Model	A	P	R	F1S	TT	M	MS
QGB	97.92	97.81	97.91	97.90	118.9128	1275.11	172.27
QSM	95.60	95.73	95.67	95.09	110.0927	1270.62	81.33
HQM	98.59	98.52	98.62	98.53	4.42	2305.43	520.49

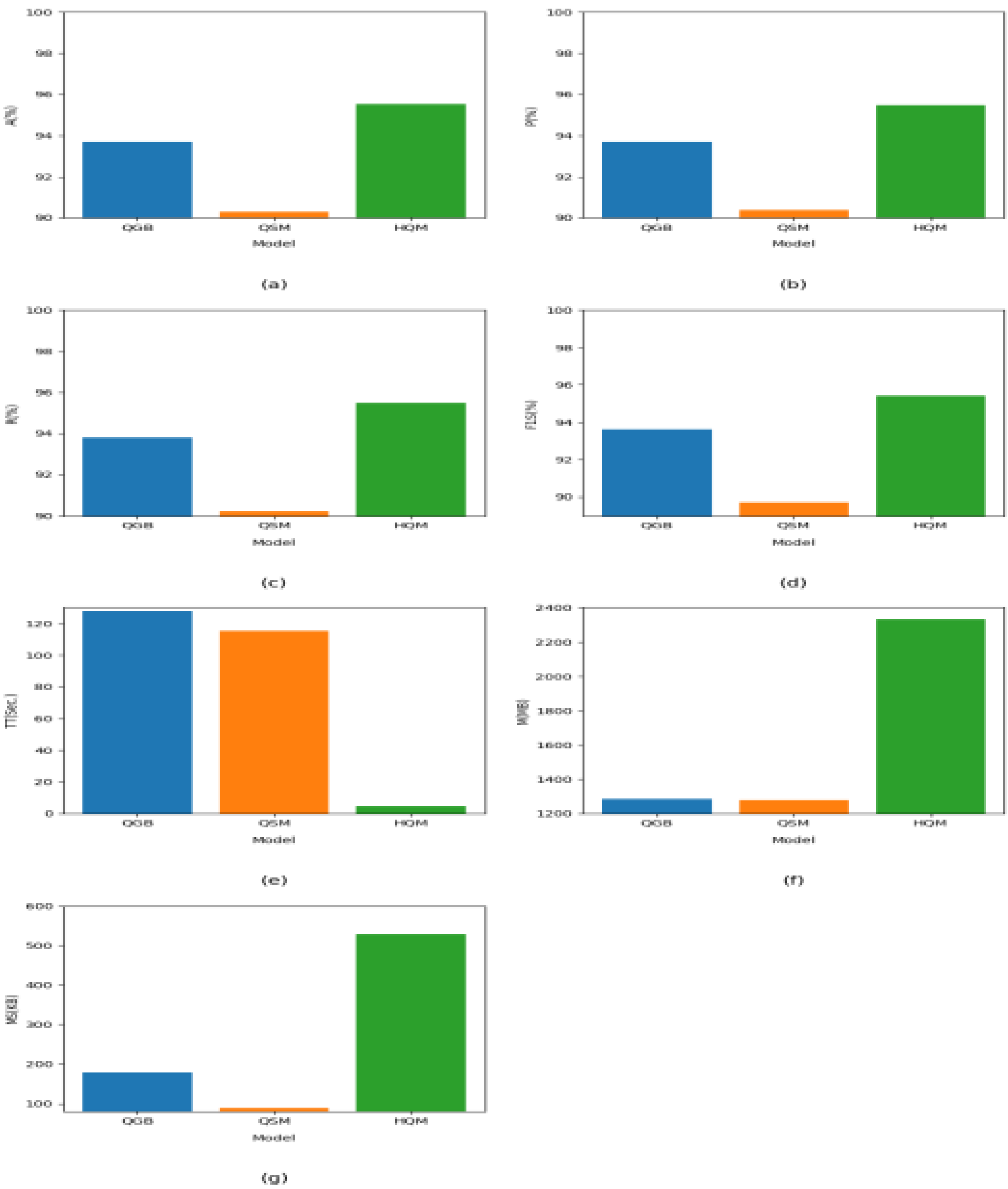

Figure 2: Graphical representation at 80 : 20 TTR before HPT

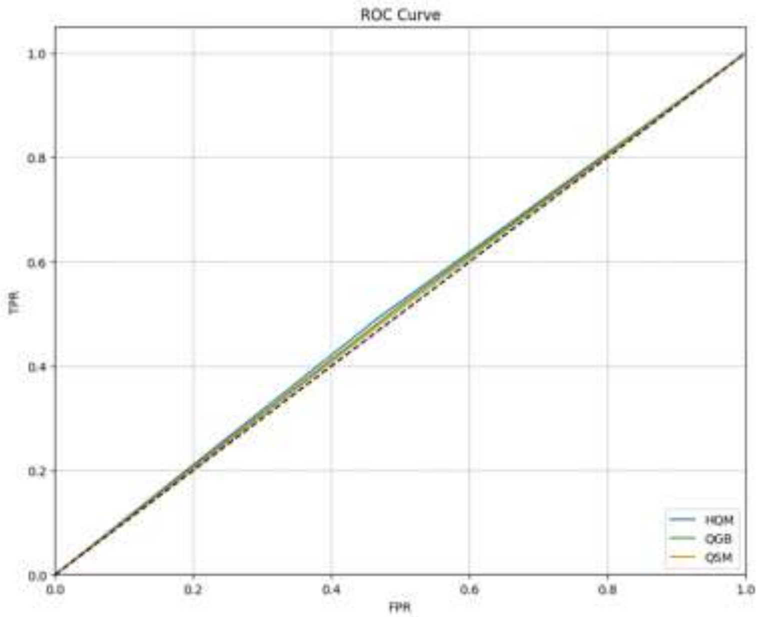

Figure 3 : ROC Curve at 80 : 20 TTR before HPT

For the 80%:20% TTR (Tables 1 - 2 and Figure 2 - Figure 3), the models QGB, QSM, and HQM are evaluated before and after HPT. Before HPT, QGB, QSM and HQM achieved the A of 93.70% 90.29% and 95.54% accordingly. HQM achieved P of 95.49% and R of 95.50%, QGB also achieved the P of 93.69% and R of 93.79% while QSM has comparatively lower P of 90.37% and R of 90.24%. The highest F1S achieved for HQM of 95.42% followed by QGB of 93.62%, and QSM of 89.71%. HQM has faster TT with 4.56 sec., with QGB at 127.82 sec. and QSM at 115.19 sec. HQM has the higher M of 2335.48 MB and MS of 528.53 KB, while QGB has 1285.19 MB and 178.39 KB, and QSM has 1276.69MB and 89.47KB. After HPT, HQM's A increased to 98.59%, QGB's to 97.92%, and QSM's to 95.60%. P for QGB to 97.81%, R to 97.91%, and F1S to 97.90%. HQM's P to 98.52%, R to 98.62%, and F1S to 98.53%, while QSM's P to 95.73%, R to 95.67%, and F1S to 95.09%. TT after HPT is reduced to 118.91 sec. for QGB, 110.09 sec. for QSM, and 4.42 sec. for HQM. M decreased for HQM to 2305.43 MB, for QGB to 1275.11 MB, for QSM to 1270.62 MB. Similarly, MS for HQM, QGB and QSM reduced to 520.49KB, 172.27 KB and 81.33 KB accordingly. TPR/FPR before HPT showed QGB with 0.75/0.00, QSM with 0.68/0.00, and HQM with 0.89/0.00. After HPT, TPR improved to 0.77 for QGB, 0.69 for QSM, and 0.91 for HQM. The ROC curve is a key metric for evaluating the performance of classifiers, particularly with respect to their ability to distinguish between positive and negative classes. In the 80%:20% TTR scenario, the ROC curve is analyzed for the models HQM, QGB and QSM both before and after HPT. All models exhibited a FPR of 0, indicating that none of the models misclassified negative instances as positive. This is reflected in the models' positions along the y-axis of the ROC curve. Before HPT, the TPR for QGB, QSM, and HQM are 0.75, 0.68, and 0.89, respectively, with HQM showing higher TPRs, indicating that it performed better in capturing TP instances compared to QGB and QSM. The ROC curve for HQM appeared higher along the curve, while QGB and QSM is positioned comparatively lower, indicating its relative underperformance. After HPT, all models showed an improvement in TPR, with QGB at 0.77, QSM at 0.69, and HQM at 0.91. This increase in TPR suggests that HQM is capable to identify TP instances after optimization. So, HQM moved further up the ROC curve, reflecting enhanced classification performance, while QGB and QSM also showed comparative improvements. Similarly, Table 3 and 4 is represented for the 70%:30% TTR before and after HPT and Table 5 and 6 is represented for the 60%:40% TTR before and after HPT.

Table 3: Results of several methods at 70 : 30 TTR before HPT

Model	A	P	R	F1S	TT	M	MS
QGB	92.31	92.32	92.43	92.32	126.51	1283.60	176.88
QSM	88.77	88.89	88.72	88.27	114.697	1273.81	88.51
HQM	94.41	94.32	94.41	94.46	4.51	2333.22	526.78

Table 4: Results of several methods at 70 : 30 TTR after HPT

Model	A	P	R	F1S	TT	M	MS
QGB	94.81	94.12	94.72	94.73	116.79	1273.76	171.13
QSM	92.31	92.48	92.36	91.89	108.81	1269.25	80.18
HQM	96.49	96.41	96.51	96.41	4.37	2304.44	518.45

Table 5: Results of several methods at 60 : 40 TTR before HPT

Model	A	P	R	F1S	TT	M	MS
QGB	91.11	91.59	91.31	91.29	125.31	1281.59	175.54
QSM	87.28	87.28	87.88	86.35	113.29	1272.73	87.63
HQM	92.31	92.18	92.50	92.67	4.39	2332.12	525.23

Table 6: Results of several methods at 60 : 40 TTR after HPT

Model	A	P	R	F1S	TT	M	MS
QGB	92.59	92.53	92.52	92.53	115.15	1272.64	170.73
QSM	91.12	91.28	91.19	90.61	107.61	1268.21	80.09
HQM	95.49	95.31	95.29	95.39	4.26	2304.39	517.43

Table 7: Average Performance Parameters Results Before HPT for several Models

Model	A	P	R	F1S	TT	M	MS
QGB	92.4	92.5	92.5	92.4	126.55	1283.46	176.94
QSM	88.8	88.9	88.9	88.1	114.39	1274.41	88.54
HQM	94.1	94.0	94.1	94.2	4.49	2333.61	526.85

Table 8: Average Performance Parameters Results After HPT for several Models

Model	A	P	R	F1S	TT	M	MS
QGB	95.1	94.8	95.1	95.1	116.95	1273.84	171.38
QSM	92.7	93.2	93.1	92.5	108.83	1269.36	80.53
HQM	96.9	96.8	96.8	96.8	4.35	2304.76	518.79

Table 7 gives the average performance parameters for these models before HPT.. HQM shows average A of 94.1%, P of 94.0%, R of 94.1%, F1S of 94.2% and TT of 4.49 sec. indicating better performance in correctly classifying positive instances. However, it requires a higher average M of 2333.61 MB and MS of 526.85 KB which is higher than both QGB and QSM. QGB achieves the moderate performance with an A of 92.4%, P of 92.5%, R of 92.5%, and F1S of 92.4%. It is also the moderate TT of 126.55 sec. and requires the M of 1283.46 MB and MS of 176.94 KB. QSM, on the other hand, provides relatively lower results with an average A of 88.8%, P of 88.9%, R of 88.9%, and F1S of 88.1%. However, it has lower TT of 114.39 sec., making it faster than QGB but slower than HQM. It uses 1274.41 MB of M and lowest MS of 88.54 KB than QGB and HQM. From the above analysis, it is observed that different models provide outputs differently depending on the performance parameters. While, HQM show better performance using the metrics such as A, P, R, F1S and TT, and QSM provides better performace using M and MS.

Table 8 gives the average performance parameters for these models after HPT. HQM shows enhanced results with an average A of 96.9%, P of 96.8%, R of 96.8%, F1S of 96.8%, and TT of 4.35 sec. indicating better performance in correctly classifying positive instances. Still, it requires a higher average M of 2304.76 MB and MS of 518.79 KB, which is higher than both QGB and QSM. QGB achieves moderate performance with an A of 95.1%, P of 94.8%, R of 95.1%, and F1S of 95.1%. It also has a moderate TT of 116.95 sec. and requires M of 1273.84 MB and MS of 171.38 KB. QSM provides relatively lower results with an average A of 92.7%, P of 93.2%, R of 93.1%, and F1S of 92.5%. However, it has lower TT of 108.39 sec. and uses 1269.36 MB of M and MS of 80.53 KB, which is lowest than both QGB and HQM. From the above analysis aftr HPT, it is observed that different models provide enhanced outputs differently depending on the performance parameters. While, HQM shows better performance using the metrics such as A, P, R, F1S, and TT and QSM provides better performance in terms of M and MS.

Table 9: Incremental results representation by applying HPT

Model	A	P	R	F1S	TT	M	MS
QGB	+4.7	+2.3	+2.6	+2.7	-9.6	-9.62	-5.56
QSM	+3.9	+4.3	+4.2	+4.4	-5.56	-5.05	-8.01
HQM	+2.8	+2.8	+2.7	+2.6	-0.14	-28.85	-8.06

Table 9 shows the incremental results after applying HPT for the models QGB, QSM, and HQM. All models exhibit significant improvements across all performance metrics. HQM shows improvements with +2.8% in A, +2.8% in P, +2.7% in R, and +2.6% in F1S. Its TT decreased by 0.14 sec., M by 28.85 MB and MS by 8.06 KB. QGB shows increase of +4.7% in A, +2.3% in P, +2.6% in R, and +2.7% in F1S. However it showa a decrease in TT by 9.6 sec., M by 9.62 MB, and MS by 5.56 KB. QSM shows improvements of +3.9% in A, +4.3% in P, +4.2% in R, and +4.4% in F1S and it achieves reductions in TT by 5.56 sec., M by 5.05 MB and MS by 8.01 KB.

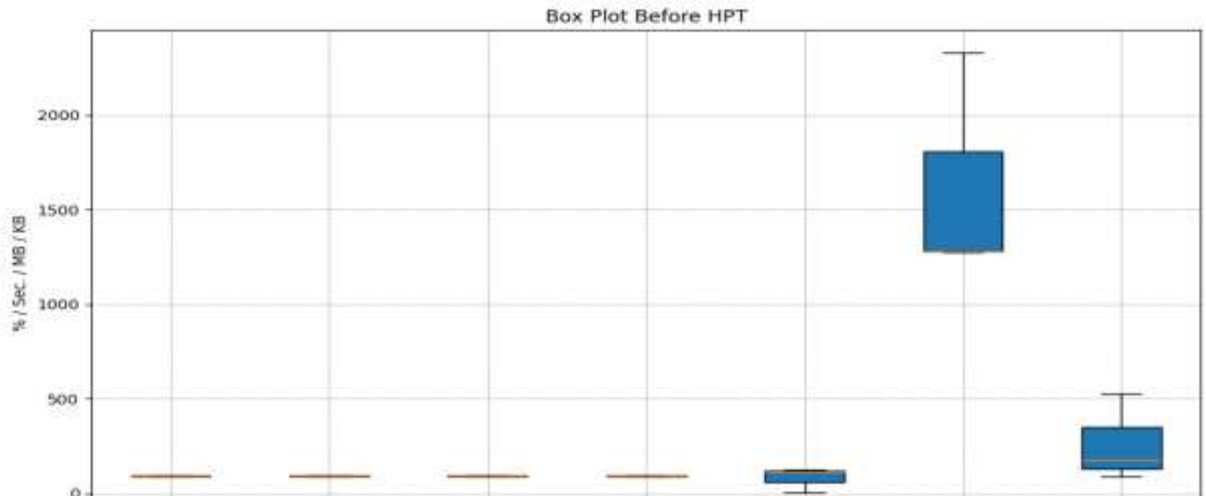

Figure 4: Boxplot before HPT

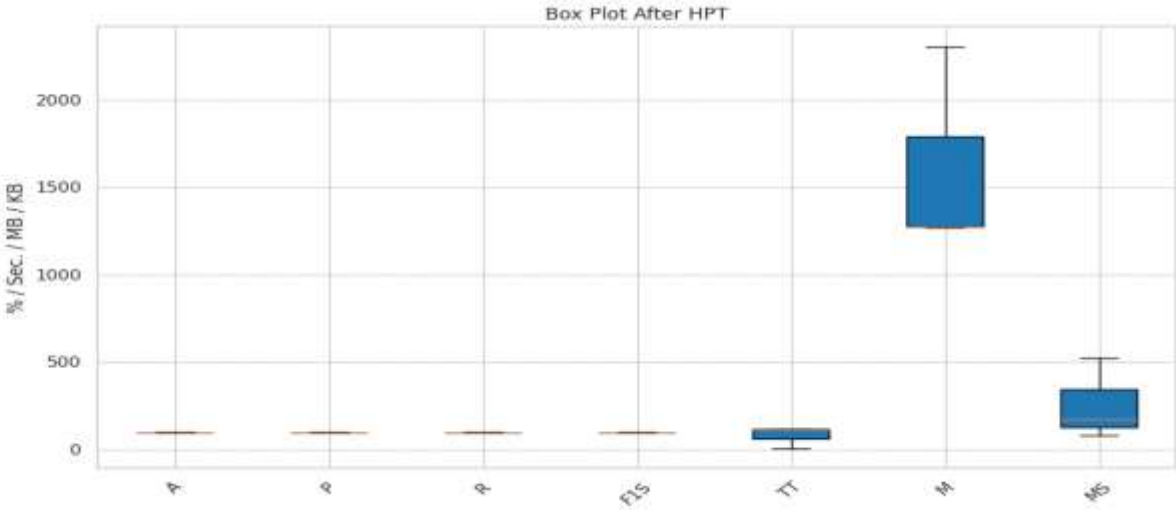

Figure 5 : Boxplot after HPT

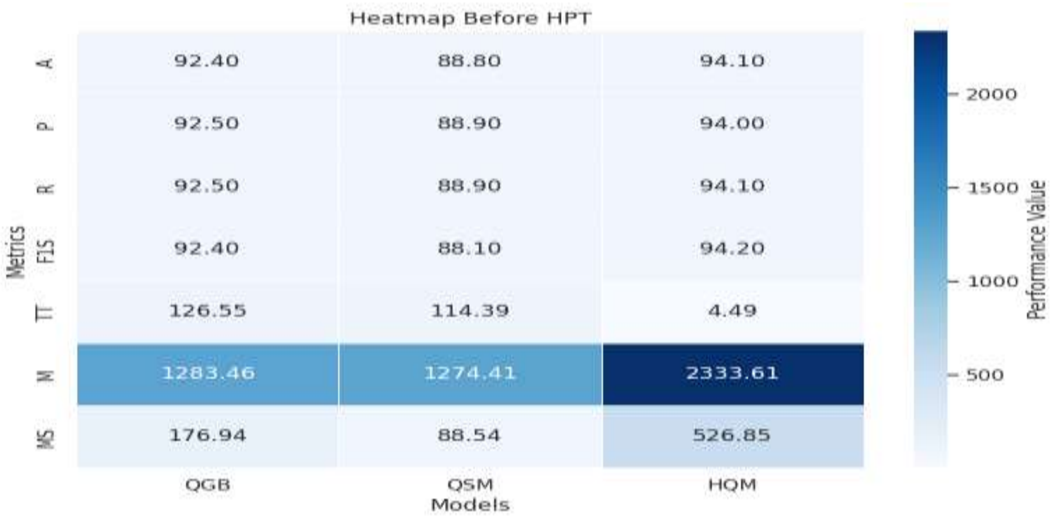

Figure 6 : Heatmap before HPT

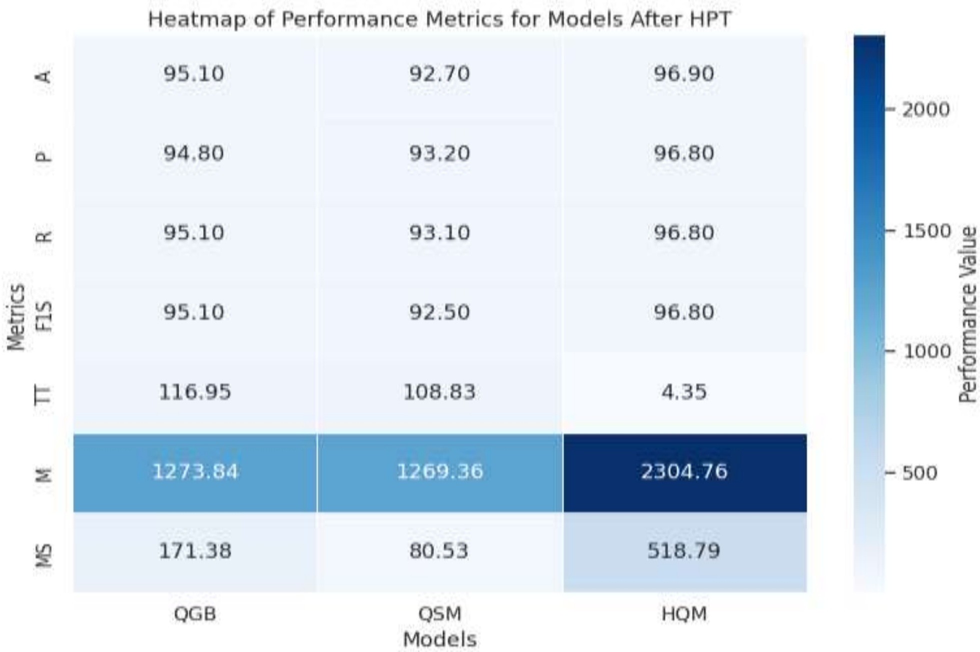

Figure 7 : Heatmap after HPT

A boxplot depicts the distribution of a D according to the key statistics such as the minimum, first quartile (Q1), median, third quartile (Q3), and maximum. It also shows potential outliers. In the Figure 4, the box plot illustrates the distribution of the average parameters such as A, P, R, F1S, TT, M, and MS before HPT and Figure 5 after HPT for the models such as QGB, QSM, and HQM. A heatmap is a graphical representation of data where individual values are represented by colors. It is used to display the relative magnitude of metrics across models. In Figure 6, the heat map shows the performance of each model across the different parameters before HPT. In Figure 7, the heat map shows the performance of each model across the different parameters after HPT.

6. STATISTICAL ANALYSIS

The ANOVA result before HPT (Table 10) shows a statistically significant difference among QGB, QSM, and HQM ($F = 583.08$, $p < 0.001$). Therefore, the models do not perform equally. HQM exhibits the highest average classification performance, whereas QSM shows the lowest.

Table 10 : ANOVA Analysis Before HPT (A, P, R and F1S)

Source	SS	df	MS	F-value	p-value
Between Groups	62.81	2	31.40	583.08	< 0.001
Within Groups	0.48	9	0.054		
Total	63.29	11			

After HPT, the ANOVA result (Table 11) again confirms a statistically significant difference among the models ($F = 349.79$, $p < 0.001$). HQM continues to provide the highest classification performance, while all models show improvement after HPT.

Table 11. ANOVA Analysis After HPT (using A, P, R and F1S)

Source	SS	df	MS	F-value	p-value
Between Groups	39.95	2	19.98	349.79	< 0.001
Within Groups	0.51	9	0.057		
Total	40.46	11			

7. CONCLUSION

The main focus of this study is to utilize QML based strategies in estimating the MHD condition of AX, DP, LL, ST and NR. The research employs three different MHD prediction models to track the MHD (QGB, QSM, HQM). All MHD Models are analysed using the following metrics: A, P, R, F1S, TT, M, and MS. Different TTR of 80:20, 70:30, and 60:40 are analysed prior and post applying HPT to all four MHD Models, and by plotting ROC, boxplot and heatmap graphs based on the metrics visualising the results. The results of this study show that HQM has the higher performance based on the metrics of: A, P, R, F1S, and TT with an average of 94.1, 94.0, 94.1, 94.2, and 4.49, respectively, pre HPT and 96.9, 96.8, 96.8, 96.8 and 4.35, respectively, post HPT. However, QSM performs better in terms of of M and MS with values 1274.41 and 88.54, and 1269.36 and 80.53 accordingly as compared QGB and HQM.This work can also be extended to apply FL based models on several D to anlyze the performance. This work can also be extended to apply edge ML based models on several D to anlyze the performance.

REFERENCES

1. Manocha A, Afaq Y, Bhatia M, “Intelligent analysis of irregular physical factors for panic disorder using quantum probability”, Journal of Experimental & Theoretical Artificial Intelligence, vol. 36, no. 7, pp. 1053–1074, 2024.
2. Singh D, Kumar GS, Agrawal S, “Quantum-inspired neurofeedback mechanism for stress detection using EEG signals”, in Real-World Applications of Quantum Computers and Machine Intelligence, IGI Global Scientific Publishing, pp. 321–336, 2025.
3. Goswami SA, Dave S, Patel KC, Raval MN, “Application of quantum artificial intelligence in healthcare”, in Quantum Computing for Healthcare Data, Elsevier, pp. 119–138, 2025.
4. Shahwar T, Rehman AU, “Automated detection of brain disease using quantum machine learning”, in Brain-Computer Interfaces, Elsevier, pp. 91–114, 2025.
5. Padha A, Sahoo A, “MAQML: A meta-approach to quantum machine learning with accentuated sample variations for unobtrusive mental health monitoring”, Quantum Machine Intelligence, vol. 5, no. 1, p. 17, 2023.
6. Gupta K, Saxena D, Rani P, Kumar J, Makkar A, Singh AK, Lee CN, “An intelligent quantum cyber-security framework for healthcare data management”, IEEE Transactions on Automation Science and Engineering, 2024.
7. Aksoy G, Cattan G, Chakraborty S, Karabatak M, “Quantum machine-based decision support system for the detection of schizophrenia from EEG records”, Journal of Medical Systems, vol. 48, no. 1, p. 29, 2024.
8. Barua PD, Kobayashi M, Tanabe M, Baygin M, Paul JK, Iype T, Dogan S, Tuncer T, Tan RS, Acharya UR, “Innovative fibromyalgia detection approach based on quantum-inspired 3LBP feature extractor using ECG signal”, IEEE Access, vol. 11, pp. 101359–101372, 2023.
9. Vasanthakumar GU, Singh M, “Quantum machine learning in healthcare: diagnostics and drug discovery”, in Quantum Machine Learning: Quantum Algorithms and Neural Networks, p. 39, 2024.
10. Shrivastava A, Kumar S, Naik NS, “Quantum leap in cardiac prognosis: EMIP-CardioPPG’s pioneering approach to early myocardial infarction prediction”, Signal, Image and Video Processing, vol. 18, no. 12, pp. 8723–8737, 2024.

11. Vaibhav Lakshmi BS, Priyalakshmi B, Elamaran E, Jahnavi M, Srivas MS, "Mental illness monitor: Integrating quantum networking and ML for physical and mental health tracking", in AI and Quantum Network Applications in Business and Medicine, IGI Global Scientific Publishing, pp. 291–310, 2025.
12. Saranya S, Menaka R, "A quantum-based machine learning approach for autism detection using common spatial patterns of EEG signals", IEEE Access, 2025.
13. Meikandan PV, Upama PB, Rabbani M, Ahamad MM, Ahamed SI, "Quantum computing for smart healthcare", in Sensor Networks for Smart Hospitals, Elsevier, pp. 525–534, 2025.
14. Alruily M, "Sentiment analysis for predicting stress among workers and classification utilizing CNN: Unveiling the mechanism", Alexandria Engineering Journal, vol. 81, pp. 360–370, 2023.
15. Kodipalli A, Fernandes SL, Dasar SK, Ismail T, "Computational framework of inverted fuzzy C-means and quantum convolutional neural network towards accurate detection of ovarian tumors", International Journal of E-Health and Medical Communications, vol. 14, no. 1, pp. 1–16, 2023.
16. Chopra S, Agarwal P, Ahmed J, Obaid AJ, "Machine-learning-based diagnosis of mental health issues", in International Conference on Information and Communication Technology for Competitive Strategies, Springer, pp. 421–430, 2023.
17. Ambika KSB, Goswami S, Pimplapure V, Jweeg MJ, Kant K, Gangodkar D, "Framework towards detection of stress level through classifying physiological signals using machine learning", in 2023 3rd International Conference on Advance Computing and Innovative Technologies in Engineering (ICACITE), IEEE, pp. 600–604, 2023.
18. Padha A, Sahoo A, "Quantum enhanced machine learning for unobtrusive stress monitoring", in Proceedings of the Fourteenth International Conference on Contemporary Computing, pp. 476–483, 2022.
19. Ullah U, Garcia-Zapirain B, "Quantum machine learning revolution in healthcare: a systematic review of emerging perspectives and applications", IEEE Access, vol. 12, pp. 11423–11450, 2024.
20. Padha A, Sahoo A, "QCLR: Quantum-LSTM contrastive learning framework for continuous mental health monitoring", Expert Systems with Applications, vol. 238, p. 121921, 2024.
21. Rahman MS, Ashik A, Rahman MS, "Comprehensive analysis of stress levels using ensemble learning and neural networks for insightful understanding", in 2024 6th International Conference on Electrical Engineering and Information & Communication Technology (ICEEICT), IEEE, pp. 1344–1349, 2024.
22. Khare SK, March S, Barua PD, Gadre VM, Acharya UR, "Application of data fusion for automated detection of children with developmental and mental disorders: A systematic review of the last decade", Information Fusion, vol. 99, p. 101898, 2023.
23. Wang FK, Kebede GA, Lo SC, Woldegiorgis BH, "An embedding layer-based quantum long short-term memory model with transfer learning for proton exchange membrane fuel stack remaining useful life prediction", Energy, vol. 308, p. 133054, 2024.
24. Hossain S, Umer S, Rout RK, Al Marzouqi H, "A deep quantum convolutional neural network based facial expression recognition for mental health analysis", IEEE Transactions on Neural Systems and Rehabilitation Engineering, 2024.
25. Tasci G, Gun MV, Keles T, Tasci B, Barua PD, Tasci I, Dogan S, Baygin M, Palmer EE, Tuncer T, et al., "QLBP: Dynamic patterns-based feature extraction functions for automatic detection of mental health and cognitive conditions using EEG signals", Chaos, Solitons & Fractals, vol. 172, p. 113472, 2023.
26. Sunki K, Reddy CKK, Reddy DMK, Doss S, "The role of quantum artificial intelligence in healthcare advancements", in Cybernetics, Human Cognition, and Machine Learning in Communicative Applications, Springer, pp. 137–158, 2025.
27. Roy AK, Jena KK, Mohapatra D, "Quantum inspired data driven fitness monitoring approach for industrial machinery", Journal of the Institution of Engineers (India): Series B, pp. 1–18, 2026.
28. Kaggle, "Mental Health Symptoms Dataset", Available: https://www.kaggle.com/datasets/rohitzaman/mental-health-symptoms-datasets. [Accessed on: Jan. 2026]